Short Communication

Effect of Ag–Co interactions in the mordenite on the NOx SCR with butane and toluene

Soledad G. Aspromonte, Eduardo E. Miró, Alicia V. Boix *

Instituto de Investigaciones en Catálisis y Petroquímica — INCAPE (FIQ, UNL — CONICET), Santiago del Estero 2829, 3000, Santa Fe, Argentina

ARTICLE INFO

ABSTRACT

A study of the lean NOx reduction activity with butane and toluene in the presence of water over bimetallic and monometallic Ag, Co exchanged on Na-mordenite catalysts was performed. The Ag–Co interactions were analyzed through X-ray photoelectron spectroscopy (XPS) and temperature-programmed reduction (TPR) techniques. It is shown that the metal silver particles formed at low temperature during the TPR experiment improve the dissociation of hydrogen thus facilitating the reduction of Co^{2+} species. The incorporation of 3.2 wt.% of silver to CoM catalyst, significantly improved the NOx to N_2 conversion with butane, which reached 95% under wet conditions (2% H_2O). However, this effect was not observed when toluene was the reducing agent.

© 2012 Elsevier B.V. All rights reserved.

1. Introduction

Nitrogen oxides (NOx), have been identified both as environmental pollutants and green house gases [1,2]. There are several sources of NOx emissions; these include fuel gases emitted by stationary and mobile sources such as lean-burn vehicles, power plants, electrical generators, nitric acid factories and biomass burning.

The selective catalytic reduction of NOx by hydrocarbons (HC-SCR) in the presence of excess oxygen is a potential method to remove NOx from several exhausts [3,4]. In the case of diesel engines, the fuel is a complex mixture of different organic compounds, among which the most important ones in the context of HC-SCR are longer chain alkanes and aromatic compounds. However, most studies of HC-SCR have been conducted using aliphatic hydrocarbons, and a few articles have focused on the effect of aromatic hydrocarbons [5–7].

Metal-zeolite based catalysts have been intensively investigate for the SCR of NOx, particularly cobalt-exchanged in mordenite, ZSM5, BEA, etc. [8–11]. On the other hand, Ag/Al_2O_3 catalysts have been the subject of numerous studies, showing promising results. This is due to their excellent ability to reduce NOx with a wide variety of the hydrocarbons (HCs) such as oxygenated hydrocarbons [12,13], and light and heavy hydrocarbons [14]. Bimetallic catalysts have also shown that the reducing activity and water resistance could be improved due to the synergetic effect between metals [15,16].

The aim of the present work is to study the effect of adding silver to Co-mordenite catalysts over the catalytic behavior in the SCR of NOx using two different HC as reducing agents, i.e. butane as saturated short chain hydrocarbon and toluene representative of the aromatic family, both present in automotive exhaust gases. The interaction between different catalytic species was determined by characterization techniques, such as, the temperature-programmed reduction (TPR) and X-ray photoelectron spectroscopy (XPS).

2. Experimental

2.1. Catalyst preparation

Zeolite mordenite was supplied in the sodium form (NaMOR) by Zeolyst International with Si/Al = 6.5 atomic ratio. The active elements (Co, Ag) were introduced by the conventional ion exchange method. First, the cobalt-exchanged Na-mordenite (CoM) catalyst was prepared using a cobalt acetate solution (0.025 M) with a ratio of 10 g of zeolite in a 1.5 L of solution. Instead, the silver-exchanged Na-mordenite (AgM) catalyst was prepared using 150 mL of 0.04 M silver nitrate solution with 4 g of NaMOR. Both exchanges were performed for 24 h at room temperature and pH between 5 and 6. Then, the solids were filtered, washed and dried at 120 °C for 8 h. The samples CoM and AgM were calcined for 4 h in air flow at a heating rate of 5 °C·min⁻¹ at 400 and 500 °C, respectively. The concentrations of cobalt and silver were 2 and 5 wt.%, respectively, which were determined by atomic absorption spectroscopy.

In the second step, the silver-exchange of the calcined CoM (AgCoM) catalyst was prepared, using a $AgNO_3$ solution (0.001 M) with a ratio of 3 g of CoM in 1 L of solution. Then, the bimetallic catalyst was calcined at 500 °C. The concentrations of cobalt and

silver were 2 and 3.2 wt.%, respectively. All the above procedures were performed in the dark due to the sensitivity of silver to light.

2.2. Catalyst characterization

Nitrogen adsorption–desorption isotherms were obtained at 77 K on a Quantachrome Autosorb instrument. Previously, the samples were outgassed at 350 °C for 6 h (10^{-4} Torr).

The cobalt and silver contents (wt.%) of the prepared catalysts were determined by atomic absorption spectroscopy.

TPR measurements were carried out using an Okhura TP-2002S instrument equipped with a TCD detector. Samples were heated at $10\ °C \cdot min^{-1}$ in inert flow up to the calcination temperature and kept constant at this temperature for 2 h. Next, they were cooled to room temperature and stabilized in H_2 (5%)/Ar. The temperature and detector signals were then continuously recorded while heating at $10\ °C \cdot min^{-1}$ up to 900 °C.

X-ray photoelectron spectra were collected using a multi-technique system (SPECS) equipped with a dual Mg/Al X-ray source and a hemispherical PHOIBOS 150 analyzer operating in the fixed analyzer transmission (FAT) mode. The spectra were recorded in the constant pass energy mode at 30 eV and the X-ray source was operated at 200 W and 12 kV. The working pressure in the analyzing chamber was less than $5 \cdot 10^{-9}$ mbar. Spectra in the Co 2p and Ag 3d regions were obtained with Al Kα (hν = 1486.6 eV) and Mg Kα (hν = 1253.6 eV) radiation, respectively. The binding energy (BE) positions of Ag 3d do not identify the oxidation state of the silver species, because the characteristic states of oxidized (Ag_2O) and metallic silver ($Ag°$) are close together (within 0.5 eV) [17]. Thus, the modified Auger parameter (α') was used to characterize the chemical state of Ag. This parameter is the sum of the kinetic energy (KE) of the Auger electron (Ag M_4VV) and the BE of the core-level (Ag $3d_{5/2}$) peak. This parameter is independent of charging, but is still sensitive to chemical shifts. The BE of core-levels Si 2p, Al 2p, Ag 3d, C 1s, O 1s, and the KE in the region of the Ag M_4VV Auger transitions were measured.

During the processing of XPS spectra, BE values were referenced to the C 1s peak (284.6 eV) from the adventitious contamination layer. All the peaks were fitted by a Gaussian–Lorentzian component waveform after and inelastic (Shirley-type) background had been subtracted in order to calculate the surface atomic ratio.

2.3. Catalytic activity measurements

The experiments were carried out at atmospheric pressure in a flow-type system designed for continuous operation. The gas composition was analyzed by a Shimadzu GC2014 gas chromatograph, equipped with a thermal conductivity detector (TCD). The HC and NO_x to N_2 conversions (X_{HC} and X_{NO}, respectively) of the catalysts on the SCR were determined between 300 and 600 °C. The reactive gas mixture was composed of 1000 ppm NO/He, 500 ppm C_4H_{10} or C_7H_8, 2% O_2, balanced at 1 atm in helium (gas-hourly space velocity, GHSV = 20,000 h^{-1}). The effect of the addition of 2 and 10% of water in the feed was also studied. The water was introduced through a saturator in which different concentrations were obtained by varying the temperature. It was kept between 20 and 22 °C achieving c.a. 2% H_2O and between 47 and 50 °C for c.a. 10% of water.

3. Results and discussion

3.1. Physical, chemical and textural properties of the catalysts

Several techniques were employed in order to determine the role of different Ag and Co species in the NO_x reduction.

Table 1 shows that the incorporation of silver and/or cobalt in the mordenite channels causes a decrease of the specific surface area (S_{BET}) and the micropore volume (V_μ) as compared with the original substrate NaMOR. The incorporation of 2 wt.% Co produces a decrease of S_{BET} close to 19%, while the V_μ remains constant. However, the addition of 5 wt.% of silver causes a loss of S_{BET} and the V_μ near 35 and 50%, respectively.

According to the metal content in the monometallic CoM and AgM samples, the ion exchange degree of Na^+ by Ag^+ or Co^{2+} ions was found to be 22 and 32%, respectively. This would indicate that the number of Ag^+ ions in the unit cell in AgM (1.4 Ag/u.c.) is greater in comparison with the number of Co^{2+} ions in the CoM sample (1.0 Co/u.c.). Furthermore, the ionic radius of the Ag^+ cation (1.26 Å) is greater than that of the Co^{2+} ions (0.74 Å). These factors could contribute to the partial blocking of the channels in the presence of Ag^+ cations. On the other hand, the AgCoM bimetallic sample was exchanged with a smaller quantity of silver (0.9 Ag^+ ions/u.c.), since the cobalt was initially present. Consequently, the surface area and pore volume decreased slightly.

3.2. Reducibility of Ag and Co species

The properties of the active centers are associated with the different species present in the catalysts. The TPR technique allows differentiating these species.

Fig. 1 shows the reduction profile obtained for the prepared catalysts and Table 1 presents the consumed hydrogen per mol of silver and/or cobalt in the mono- and bimetallic catalysts.

Three different temperature regions attributed to different species are observed. The calcined CoM (Fig. 1, profile a) presents a small peak at 78 °C in addition to two other peaks, one between 300 and 450 °C and another with a maximum at 721 °C. For the temperatures lower than 600 °C, the H_2/Co molar ratio is c.a. 0.07, which could correspond to the reduction of 7% of CoO (Co^{2+}) or 5.2% of Co_3O_4 species, while the peak at higher temperature is due to the reduction of 44% of Co^{2+} ions at exchange positions in the channels of Na-mordenite [18]. The total consumption of hydrogen per mol of cobalt is equal to 0.51, indicating that a fraction of Co^{2+} ions is at very stable sites within the structure and that it is not reduced (Table 1).

The calcined AgM (Fig. 1, profile b) shows two peaks below 300 °C which are associated with the reduction of small particles of highly dispersed Ag_2O [19]. The micromoles of consumed H_2 indicate that 28% of the overall silver is reduced at lower temperature. Also, the reduction between 300 and 600 °C with a maximum at 406 °C is linked to a fraction of Ag^+ (34%) ions at exchange positions within the zeolite. Furthermore, there is a small peak above 600 °C which can be assigned to the reduction of 10% of Ag^+ cations located at more stable sites in the mordenite structure like the side pockets [20]. The number of micromoles of hydrogen consumed represents a reduction of 72% of the silver present in the catalyst, which indicates that there is a fraction, close to 28%, that is not reduced in the temperature range studied (Table 1).

Table 1
Textural properties and TPR results obtained for NaMOR exchanged with Ag and/or Co.

Catalysts[a]	S_{BET}[b] ($m^2 \cdot g^{-1}$)	V_μ[c] ($cm^3 \cdot g^{-1}$)	H_2/(Ag + Co)[d]	% reduction[e]	
				Ag	Co
NaMOR	409	0.165	–	–	–
Co(2)M	332	0.166	0.51	–	51
Ag(5)M	265	0.083	0.36	72	–
Ag(3.2)Co(2)M	310	0.150	0.68	100	74

[a] The numbers between parentheses indicate the weight percentage of the metals.
[b] Specific surface area calculated from the N_2 adsorption isotherms at −196 °C ($m^2 \cdot g^{-1}$).
[c] Micropore volume calculated from the t-plot method ($cm^3 \cdot g^{-1}$).
[d] H_2 consumption per mol of silver and cobalt obtained by temperature-programmed reduction.
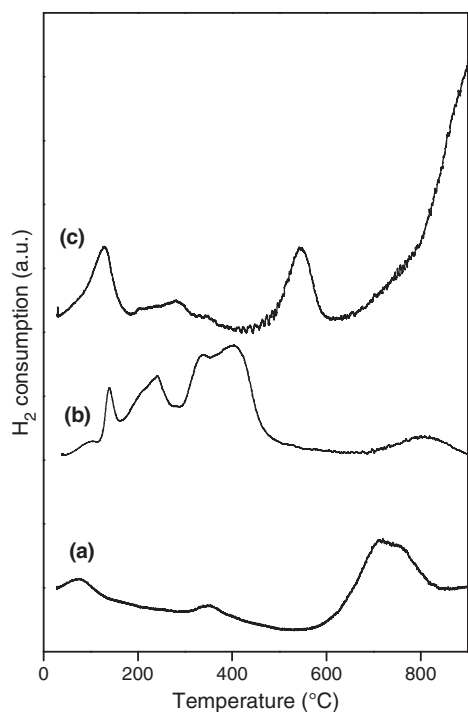[e] Percentage of reduction referred to Co^{2+} or Ag^+ species.

Fig. 1. TPR profiles obtained for calcined (a) Co(2)M, (b) Ag(5)M and (c) Ag(3.2)Co(2) M catalysts.

Table 2
XPS analysis and modified Auger parameter.

Catalysts	BE (eV)[a]		KE (eV)[b]	α'^c
	Co 2p$_{3/2}$	Ag 3d$_{5/2}$	Ag M$_4$VV	
Co(2)M	781.9 (4.1)[d]	–	–	–
Ag(5)M	–	368.4 (2.1)	354.0 (4.0)	722.4
Ag(3.2)Co(2)M	781.9 (3.4)	368.6 (2.1)	354.1 (3.8)	721.7

[a] Binding energy of the Co 2p$_{3/2}$ and Ag 3d$_{5/2}$ region (eV).
[b] Kinetic energy of the Auger region (eV).
[c] Modified Auger parameter, α' (eV) = KE (Ag M$_4$VV) − KE (Ag 3d$_{3/2}$) + 1253.6 eV.
[d] fwhm: full width at half maximum (eV).

It is observed that the reduction profile obtained for the bimetallic sample (Fig. 1, profile c) does not correspond to the sum of the profiles obtained for the monometallic samples.

The AgCoM sample presents one reduction peak at 160 °C with another broad peak with a maximum at 282 °C, which could be assigned to the overlapped reduction of Ag$_2$O and CoO$_x$ species. With the presence of Ag in CoM, the reduction peak of the Co$_3$O$_4$ species shifted from 356 °C to temperatures below 300 °C, as shown in Fig. 1. There is another peak between 400 and 600 °C that corresponds to a fraction of Co^{2+} or Ag$^+$ cations exchanged in the Na-mordenite structure [21]. A continuous increase of the H$_2$ consumption above 650 °C is also observed.

The measured hydrogen consumption for AgCoM between 130 and 600 °C (Table 1) would indicate that a larger proportion of cobalt species than that observed in the monometallic samples is reduced at lower temperatures. Taking into account that all silver species present in the solid are reduced at the above mentioned temperature range, it is possible to assume that 25% of Co$_3$O$_4$ is simultaneously reduced. In addition, 44% of cobalt (as Co $^{2+}$ ions) is reduced at 556 °C. The remaining fraction of Co^{2+} ions located at very stable positions within the mordenite framework (γ sites) is reduced above 650 °C. Thus, it is clear that the redox behavior of cobalt ions in the mordenite structure is altered by Ag$^+$ ions. Consequently, the reduction of cobalt species is promoted due to the strong interaction between Ag and Co species. In addition, it is possible that the metal silver particles, formed at low temperatures during the TPR experiment, improves the dissociation of hydrogen and facilitates the reduction of Co^{2+} species.

It is also possible to consider that the addition of silver to the CoM sample allows the formation of mixed oxides Ag$_x$Co$_y$O$_z$ with properties that are different from those of pure oxides. This effect together with the proximity of the Co^{2+} and Ag$^+$ cations in the cavities of the mordenite contributes to a synergism between the two metals.

3.3. Surface species

The XPS technique was applied to determine the oxidation state of Ag and/or Co present in the surface of the samples. The XPS results obtained are shown in Table 2.

In the monometallic (CoM) and bimetallic (AgCoM) samples, the Co 2p$_{3/2}$ peak position is found around 781.9 eV, with a spin-orbit splitting at 797.9 eV, corresponding to the Co 2p$_{1/2}$ peak. The main peak is accompanied by a relatively intense 3d → 4 s *shake-up* satellite peak at 787.4 eV, which is characteristic of Co^{2+} species. In agreement with literature results, these binding energy values are characteristic of Co^{2+} at exchange position on Co-zeolites [11].

On the other hand, the more intense XPS signal for silver corresponds to the 3d electronic level, which presents a characteristic doublet 3d$_{3/2}$–3d$_{5/2}$, with a spacing of 6 eV. However, it is difficult to distinguish differences in the oxidation states of silver considering only the binding energy of Ag 3d. Accordingly, the Ag$_2$O (367.8 eV), AgO (367.4 eV) and Ag° (368.2 eV) species exhibit an almost similar BE value in this region [22]. For this reason, the KE of the transition Auger Ag M$_4$VV was measured and thus, the modified Auger parameter α' was calculated (Table 2). The α' values reported in the literature for Ag° and Ag$_2$O are distinctly different, 726.3 and 724.5 eV, respectively [23]. Parameters α' of AgM and AgCoM were 722.4 and 721.7 eV, respectively.

The first value confirms that the Ag$^+$ ions are located in mordenite with a different environment, surrounded by the oxygen atoms of the structure, which do not correspond to Ag$_2$O oxide or Ag° species. The decrease of the α' value in AgCoM is indicative of the interaction between silver and cobalt ions. The surface atomic ratios Co/Si and Ag/Si are 0.04 and 0.11 for the monometallic catalysts CoM and AgM, respectively. A decrease of both relationships for the AgCoM sample is detected. Further, the binding energies of Si 2p and Al 2p core level spectra for all samples are 102.6 and 74.1 eV, respectively.

3.4. Catalytic behavior

The catalytic activity of the CoM, AgM and AgCoM catalysts was evaluated in HC-SCR using two different hydrocarbons: butane as an unsaturated short chain hydrocarbon and toluene as a representative of the aromatic family.

The conversions to N$_2$ achieved with the AgM catalyst and using butane as a reductant are 30 and 35% in dry and wet conditions, respectively. No improvement in NO$_x$ conversion is observed when toluene is used (Fig. 2).

On the contrary, under dry conditions and using butane, the monometalic CoM catalyst has a maximum conversion to nitrogen of 51%, which increases to 69% when the reducing agent is toluene (Fig. 3).

The CoM catalyst exhibits higher activity for NO reduction than the AgM sample, which could indicate that the Co^{2+} ions are more active than the Ag$^+$ species.

The incorporation of 3.2 wt.% of silver to the CoM catalyst produces an increase of the conversion to N$_2$, which reaches 74% with butane under dry conditions (Fig. 4). This increase is not observed when toluene is used as a reductant (Fig. 5). Besides, for all catalysts, the butane or toluene conversion is close to 100% when the NO$_x$ conversion is maximum.

It is noted that the temperature of the maximum conversion of NO$_x$ to N$_2$ is higher when toluene is used as reducing agent. It should
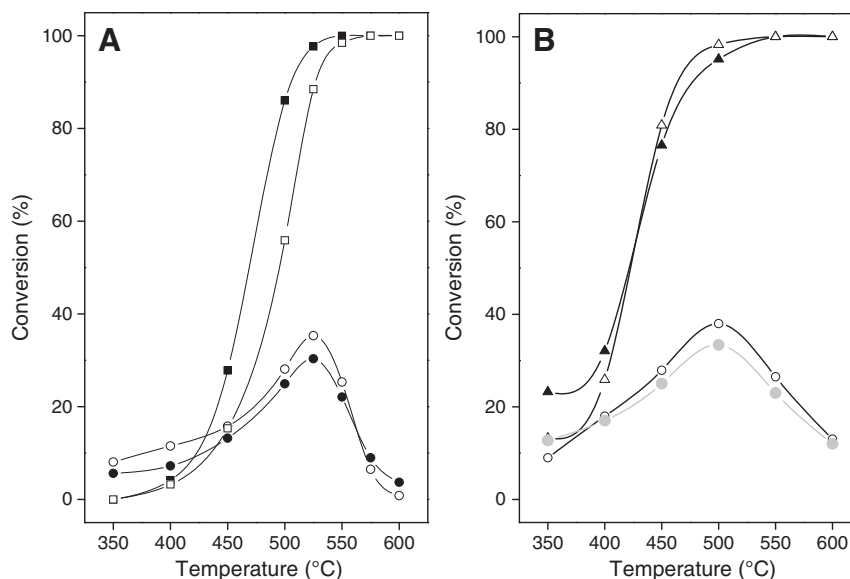
Fig. 2. HC-SCR of NO$_x$ on AgM catalyst using C$_4$H$_{10}$ (A) or C$_7$H$_8$ (B). (●, ○) NO to N$_2$, (■, □) C$_4$H$_{10}$ or (▲, △) C$_7$H$_8$ and conversions. Reaction conditions: 2% O$_2$, 1000 ppm NO, 20,000 h^{-1} and 500 ppm C$_4$H$_{10}$ or C$_7$H$_8$. Filled symbols: dry conditions; empty symbols: 2% H$_2$O.

also be considered that the C/N ratio is 3.5 or 2 when using toluene or butane, respectively. Thus, the trends in the NO$_x$ activity suggest that coke deposition on the catalysts surface depends on the C/N ratio and the hydrocarbon nature. In our previous work, we reported that the NO to N$_2$ conversion reached 60% on Co(2.9%)MOR using butane. After 30 h on stream with 2% of water, it remained constant. In contrast, a slight deactivation in dry conditions could be detected [11]. In the case of toluene, there is probably a dominant effect of coking at low temperature [24,25].

Furthermore, there is an improvement of NO$_x$ conversion to N$_2$ for all samples with the addition of 2% H$_2$O in the feed stream either with toluene or butane. Monometallic AgM and CoM catalysts show a slight increase in the conversion of NO$_x$ to N$_2$ under wet conditions. However, for the bimetallic catalyst the reducing activity promotion

is more significant. Figs. 4 and 5 show the effect of 2 and 10% of water vapor on the conversion of the AgCoM catalyst using butane or toluene, respectively.

The pore size of the mordenite used in this work (6.5 × 7 Å) allowed the cationic exchange of both Ag$^+$ (1.26 Å) and Co^{2+} (0.74 Å) ions, thus making the Co–Ag synergy possible. On the other hand, the kinetic diameters of butane (4.3 Å) and toluene (5.8 Å) are small enough for the diffusion of these molecules inside mordenite crystals, which indicates that SCR reaction occurs not only at the crystals external surface but also inside the mordenite pores.

The incorporation of silver in the CoM catalyst improves the maximum nitrogen conversion to 95 and 56% with butane and toluene, respectively, in the presence of 2% H$_2$O. It has been reported that the activity of SCR by long chain alkanes increases in the presence
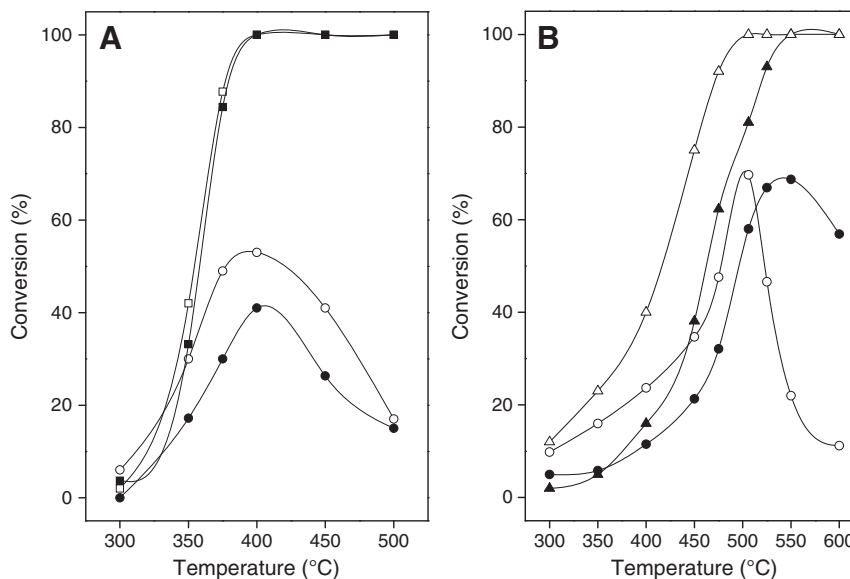

Fig. 3. HC-SCR of NO$_x$ using CoM catalyst using C$_4$H$_{10}$ (A) or C$_7$H$_8$ (B). (●, ○) NO to N$_2$, (■, □) C$_4$H$_{10}$ or (▲, △) C$_7$H$_8$ and conversions. Reaction conditions: 2% O$_2$, 1000 ppm NO, 20,000 h^{-1} and 500 ppm C$_4$H$_{10}$ or C$_7$H$_8$. Filled symbols: dry conditions; empty symbols: 2% H$_2$O.
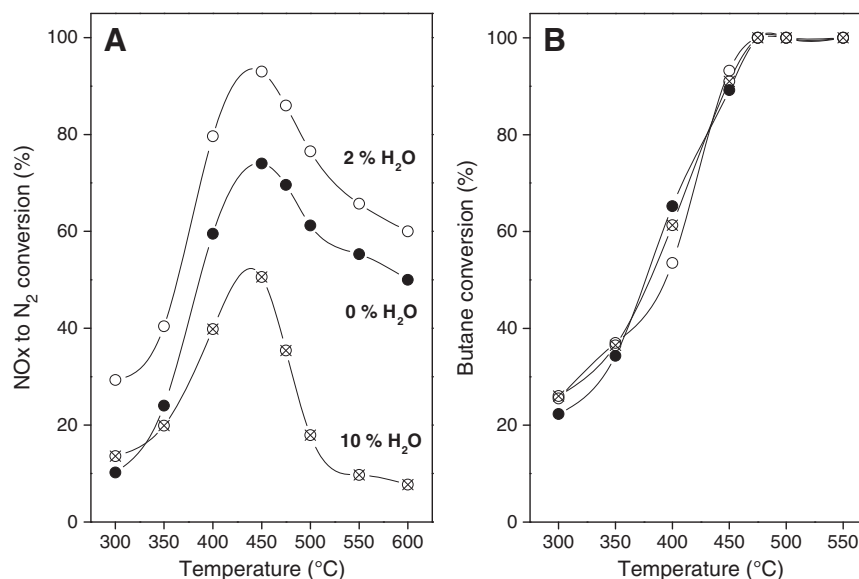
Fig. 4. Curves of (A) NO_x to N_2 and (B) butane conversions versus temperature obtained for AgCoM catalysts. Reaction conditions: 2% O_2, 1000 ppm NO, 500 ppm C_4H_{10}, 20,000 h^{-1}, (●) 0%, (○) 2% and (⊗) 10% H_2O.

of water due to the decrease in the concentration of carbonaceous species which block adsorption sites at the surface [26,27].

The catalytic performance in the HC SCR of NO_x of catalysts based on silver depends on the Ag contents. In a previous work, the effect of the content of Ag in AgM catalysts from 0.15 to 15 wt.% was reported [24]. The maximum NO_x to N_2 conversion has an optimum value between 5 and 10 wt.% in dry conditions and this conversion increases with the addition of 2% of water in the reaction mixture. However, in this case the AgM catalyst has a higher silver content (5 wt.%) than the bimetallic AgCoM (3.2 wt.% Ag) and is less active (see Figs. 3 and 4). Therefore, the predominant effect is due to the interaction between silver and cobalt species.

However, the addition of 10% H_2O in the feed stream decreases the reducing activity with both hydrocarbons. The partial deactivation is usually attributed to the water adsorption on active sites. Consequently, when the concentration of water is higher, the competitive

adsorption of water and NO molecules on active metal sites of AgCoM explains the decrease in catalytic activity.

4. Conclusions

It has been shown that the incorporation of 3.2 wt.% of silver to the CoM catalyst promotes the conversion of NO_x to N_2, which reaches 95% with butane under wet conditions (2% H_2O), effect that is not observed when toluene is the reducing agent. On the other hand, the TPR experiments show that the presence of Ag enhances the reducibility of Co ions, probably because the metal silver particles formed at low temperature improve the dissociation of hydrogen. These results could be responsible for the enhanced activity when butane is used. The different behaviors observed when using toluene can be ascribed to the different reaction mechanisms carried out with
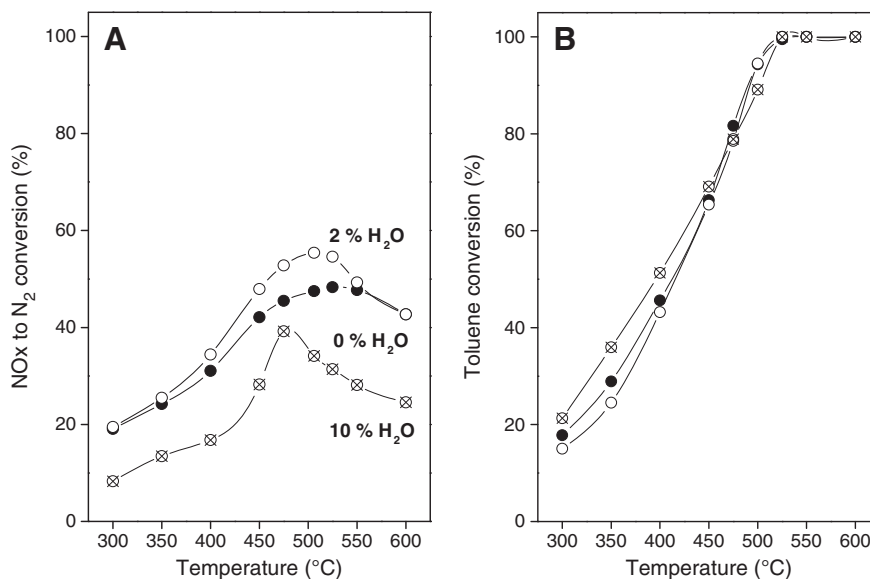

Fig. 5. Curves of (A) NO_x to N_2 and (B) toluene conversions versus temperature obtained for AgCoM catalysts. Reaction conditions: 2% O_2, 1000 ppm NO, 500 ppm C_7H_8, 20,000 h^{-1}, (●) 0%, (○) 2% and (⊗) 10% H_2O.

aromatic hydrocarbons. Further experiments are in progress to better understand this issue.

Acknowledgments

References

[1] G.A. Rhys-Tyler, W. Legassik, M.C. Bell, Atmospheric Environment 45 (2011) 3285–3293.
[2] R. Monastersky, Nature 458 (2009) 1091–1094.
[3] M. Iwamoto, H. Hamada, Catalysis Today 10 (1991) 57–71.
[4] W. Held, A. Koenig, L. Puppe, Zeolites 11 (1991) 411.
[5] Y. Li, J.N. Armor, Applied Catalysis B: Environmental 1 (1992) L31–L40.
[6] J.M. García-Cortés, J. Pérez-Ramírez, M.J. Illán-Gómez, F. Kapteijn, J.A. Moulijn, C. Salinas-Martínez de Lecea, Applied Catalysis B: Environmental 30 (2001) 399–408.
[7] I.O. Costilla, M.D. Sánchez, M.A. Volpe, C.E. Gígola, Catalysis Today 172 (2011) 84–89.
[8] M. Iwamoto, Studies in Surface Science and Catalysis 60 (1991) 327–334.
[9] E.M. Sadovskaya, A.P. Suknev, L.G. Pinaeva, V.B. Goncharov, B.S. Balazhinimaev, C. Chupin, J. Pérez-Ramírez, C. Mirodatos, Journal of Catalysis 225 (2004) 179–189.
[10] M.C. Campa, I. Luisetto, D. Pietrogiacomi, V. Indovina, Applied Catalysis B: Environmental 46 (2003) 511–522.
[11] A.V. Boix, S.G. Aspromonte, E.E. Miró, Applied Catalysis A: General 341 (2008) 26–34.
[12] T. Furusawa, K. Seshan, J.A. Lercher, L. Lefferts, K. Aika, Applied Catalysis B: Environmental 37 (2002) 205–216.
[13] R. Zhang, S. Kaliaguine, Applied Catalysis B: Environmental 78 (2008) 275–287.
[14] V. Houel, P. Millington, R. Rajaram, A. Tsolakis, Applied Catalysis B: Environmental 73 (2007) 203–207.
[15] L. Guczi, D. Bazin, Applied Catalysis A: General 188 (1999) 163–174.
[16] L. Gutierrez, E.A. Lombardo, Applied Catalysis A: General 360 (2009) 107–119.
[17] J.T. Wolan, G.B. Hoflund, Applied Surface Science 125 (1998) 251–258.
[18] A. Boix, E.E. Miró, E.A. Lombardo, M.A. Bañares, R. Mariscal, J.L.G. Fierro, Journal of Catalysis 217 (2003) 186–194.
[19] H. Berndt, M. Ritcher, T. Gerlach, M. Baerns, Journal of the Chemical Society, Faraday Transactions 94 (1998) 2043–2046.
[20] W.J. Mortier, Journal of Physical Chemistry 81 (1977) 1334–1338.
[21] A. Westermann, B. Azambre, A. Koch, Catalysis Today (2012), http://dx.doi.org/10.1016/j.cattod.2011.12.030.
[22] X.Y. Gao, S.Y. Wang, J. Li, Y.X. Zheng, R.J. Zhang, P. Zhou, Y.M. Yang, L.Y. Chen, Thin Solid Films 455 (2004) 438–442.
[23] S. Bera, P. Gangopadhyay, K.G.M. Nair, B.K. Panigrahi, S.V. Narasimhan, Journal of Electron Spectroscopy and Related Phenomena 152 (2006) 91–95.
[24] S.G. Aspromonte, E.E. Miró, A.V. Boix, Applied Catalysis A: General 407 (2011) 134–144.
[25] V. Houel, P. Millington, R. Rajaram, A. Tsolakis, Applied Catalysis B: Environmental 77 (2007) 29–34.
[26] S.G. Aspromonte, E.E. Miró, A.V. Boix, Adsorption 18 (2012) 1–12.
[27] B.P.M. Holbrook, A. Baylet, L. Retailleu, A. Boreave, P. Vernoux, F. Figueras, A. Giror-Fendler, Catalysis Today 176 (2011) 48–55.